Functional Biomaterials Surfaces

JOURNAL OF
biomaterials applications

Journal of Biomaterials Applications
2016, Vol. 31(5) 784–796

DOI: 10.1177/0885328216671239
jba.sagepub.com
SAGE

Fabrication and characterization of metal stent coating with drug-loaded nanofiber film for gallstone dissolution

Qiang Gao[1], Chao Huang[2], Binbin Sun[1], Bhutto M Aqeel[1], Jing Wang[1], Weiming Chen[1], Xiumei Mo[1,3*] and Xinjian Wan[2*]

Abstract

Stent insertion and chemical agents of ethylene diamine tetraacetic acid and sodium cholate for dissolving common bile duct stone diseases through extra biliary tract infusion have been believed a relatively effective therapeutics for the clinical symptom. Core-shell nanofibers produced by co-axial electrospinning to deliver chemical drugs, biomacromolecules, genes and even cells have been reported for various advanced drug delivery system and tissue engineering applications. In the present study, poly (lactide-co-ε-caprolactone) (PLCL) core-shell nanofiber-coated film of stent, loaded with ethylene diamine tetraacetic acid and sodium cholate in core layer, was fabricated by co-axial electrospinning for treating gallstone disease. Image of laser scanning confocal microscopy and transmission electron microscopy demonstrated core-shell structure of drug-loaded nanofiber. Fourier transform infrared spectra and the thermogravimetric analysis proved ethylene diamine tetraacetic acid and sodium cholate to be successfully loaded in nanofibers. Morphology of nanofibers after a period of degradation still keeps good shape. Drugs can continuously release for around five days, which was proved significant effectiveness for dissolving gallstone. Besides, unobvious cytotoxicity was exhibited from MTT results and cell kept good morphology in vitro research. The present coated stent showed a bright prospect for dissolving the biliary stone.

Keywords

Co-axial electrospinning, nanofiber, ethylene diamine tetraacetic acid and sodium cholate, poly (lactide-co-ε-caprolactone), release, gallstone

Introduction

Common bile duct (CBD) stones, also known as gallstones, are the most CBD disease and can be successfully treated with stone extraction using by conventional endoscopic sphincterotomy method. However, 10–20% of gallstones could not be removed due to large numbers, large size, or anatomic abnormality.[1,2] The traditional treatments of choleretic agents such as ursodeoxycholic acid can decrease stone size through oral agent or bile duct perfusion and improve extraction success rate.[3–5] As an effective bridge therapy for CBD stones, insertion of a temporary stent achieves a successful rate of gallstone removal varying from 44% to 92%.[6] In addition, drug-eluting stents reported in some studies have better outcomes for gallstone compared to stents alone.[7,8]

Electrospinning technology is a convenient and versatile method for fabricating multifunctional nanofibers from natural and synthetic polymers or their composites,[9–11] which has attracted wide attention of researchers in the field of nanotechnology, especially in fabrication of nanomaterial. In the last two decades, with rapid development of manufacturing industry and nanotechnology, classical electrospinning has also

[1]State Key Laboratory for Modification of Chemical Fibers and Polymer Materials, College of Chemistry, Chemical Engineering and Biotechnology, DongHua University, Shanghai, China
[2]Department of Gastroenterology, First People's Hospital, Shanghai Jiaotong University, School of Medicine, Shanghai, China
[3]Shandong International Biotechnology Park Development Co., Ltd, Shandong, China

Corresponding authors:
*Xiumei Mo, State Key Laboratory for Modification of Chemical Fibers and Polymer Materials, College of Chemistry, Chemical Engineering and Biotechnology, DongHua University, Shanghai 201620, China.
Email: xmm@dhu.edu.cn
*Xinjian Wan, First People's Hospital, Shanghai Jiaotong University, School of Medicine, Shanghai 201620, China.
Email: Wanxj99@163.com

made considerable progress and is divided into blend electrospinning, needleless electrospinning, emulsion electrospinning, side-by-side electrospinning, coaxial electrospinning, and dynamic liquid electrospinning.[12–17] Electrospun nanofibers showed excellent properties such as fabulous mechanical performance, porous structure, high surface-area-to-volume ratio, and mimicking to biological nanofibrous configuration of the native extracellular matrix (ECM). Such excellent characteristics of electrospun nanofibers make them most suitable applicant for various fields, such as adsorbent and catalyst,[11,18] photoelectric conversion and energy storage,[19] biological detection,[20] biosensors,[21] drug delivery,[22] tissue engineering[23,24] and have brought huge economic benefits to society. Nanofibers as a reservoir for storing drugs have a bright prospect in controlling drug release and some new nanofiber drug delivery system (DDS) have attracted more attention towards sustained and stable release of drug which is crucial to maximum therapeutic effectiveness and minimum potential toxicity.

Poly (lactide-co-ε-caprolactone) (PLCL) is a biodegradable nontoxic copolymer composites of L-lactide (LA) and ε-caprolactone (CL). PLCL possess very diverse mechanical and degradation rate properties depending on the ratio of LA and CL.[25,26] Moreover, PLCL is harmless to animals and is approved by the Food and Drug Administration (FDA), and has been extensively used in drug release and tissue engineering applications. Ethylene diamine tetraacetic acid (EDTA) is the most classic chelating agent for most metal ions and widely used as chelating agents, detergent and blood anticoagulant applications.[27–29] As a powerful chelating agent for calcium bilirubinate, some researchers have used EDTA as dissolving agent for treating calcium bilirubinate gallstone with the method of biliary infusion techniques.[30,31] Sodium cholate (SC) normally obtained from animal bile juices is a kind of cholate mixture and has the potency to dissolve cholesterol stones. Sohrabi et al.[32] have reported its role in dissolving gallstones through extra hepatic biliary tract infusion in previous study.

Metal stent coating with drug-loaded electrospun nanofiber is intended to be inserted into biliary suffering from gallstones though gastrointestinal gndoscopy for dissolving gallstone. Meanwhile, the lumen of stent keeps bile flowing fast. Until now, no study has been reported on drug-eluting stent-wrapped PLCL nanofibers loaded with EDTA&SC for dissolving biliary stones. In this study, under the same injected rate condition of shell layer, nanofiber film loaded with various amount of drugs coating on stent was fabricated by co-axial electrospinning via controlling different core-injected rate and further characterized for its physiochemical properties and continuous drugs releasing profile in PBS solution. Present metal stent coating with drug-loaded electrospun nanofiber had a continuous release time of about five days and displayed a satisfying result in dissolving gallstone in vitro analysis. All these data on coated stent paved way for later clinical application to evaluate the efficiency for biliary stone dissolution.

Experimental

Materials and reagents

The co-polymer of PLCL (Mw = 300 kDa, PLA: PCL = 50:50) was supplied by Jinan Daigang Biomaterial Co., Ltd, China. EDTA was purchased from Sinopharm Chemical Reagent Co., Ltd, China and SC was obtained from J & K Technology Co., Ltd, China. The nitinol stent was provided by Micro-Tech Co., Ltd, China. The solvent of 1, 1, 1, 3, 3, 3-Hexafluoro-2-propanol (HFIP) was purchased from Shanghai Darui Finechemical Co., Ltd, China. Fluorescein isothiocyanate-conjugated bovine serum albumin (FITC–BSA) was purchased from Invitrogen (Carlsbad, CA, USA). All the reagents for cell culture including fetal bovine serum (FBS), horse serum (HS), Dulbecco's modified Eagle's medium (DMEM), phosphate-buffered saline (PBS), trypsin/EDTA, RPMI 1640 medium and penicillin–streptomycin were purchased from Gibco BRL, Life Technologies, USA. Pig iliac endothelium cell lines (PIEC) were supported by Shanghai Institute of Biochemistry and Cell Biology (SIBCB, CAS, China).

Fabrication of coated stent

The electrospinning solution (12 w/v%) for shell layer was prepared by dissolving PLCL in HFIP, and drugs of 1:1 molar ratio EDTA and SC were dissolved in ultra-pure water for core layer solution (31 w/v%) at room temperature. Different amount of drugs' core-shell nanofibers were obtained though controlling the injected rate of inner layer, and ultimately the theoretical ratio of drugs and PLCL materials is listed in Table 1.

Stents coating with drug (ECTA&SC)-loaded nanofiber film were fabricated by co-axial electrospinning and collected with a rotated equipment (Figure 1). Briefly, two syringes containing two sorts of solutions of drugs and PLCL material were separately loaded in two syringe pumps (789100C, Cole-Parmer Instruments, USA) and connected with two capillaries to a special co-axial stainless steel needle consisting of an inner 21 G needle and an outer 30 G needle, and the inner tip protruded 0.5 mm from the outer one, in which the shell solution was injected at the flow rate of 2 mL/h

Table 1. Manufacturing parameter of drug-loaded nanofiber coated on stents.

Nanofiber coating on stent	Voltage	Distance	Rotated rate of collector	Electrospinning time	Ratio of EDTA&SC and PLCL (w/w)	Percentage of EDTA&SC in drug-loaded nanofibers (w/w)	Injected rate of shell layer	Injected rate of core layer
PLCL-W[a]	10 kV	15 cm	120 r/min	30 min	0%	0%	2 mL/h	0.24 mL/h
PLCL-D-10					10%	9.1%		0.08 mL/h
PLCL-D-30					30%	23.1%		0.24 mL/h
PLCL-D-50					50%	33.3%		0.40 mL/h
PLCL-D-60					60%	37.5%		0.48 mL/h

[a]Core layer solution is ultra-pure water in PLCL-W nanofibers.

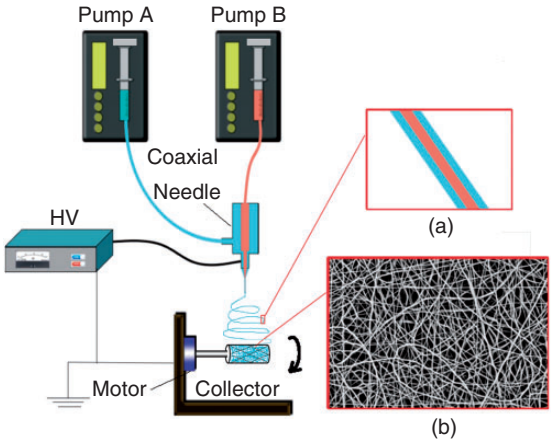

Figure 1. Schematic illustration of prepared process for coated stent by co-axial electrospinning. (a) Structure of single core-shell nanofiber, (b) actual SEM image of nanofibers.

meanwhile the injected rate of core solution fed are given in Table 1. Taylor's cone was elongated to form nanofiber in the electric field. Ultimately, nanofibers fell off rotated stent to obtain integrated coated stent.

Characterization

Morphology and diameter of nanofibers

Nanofiber morphology of samples was observed with a scanning electron microscope (SEM, Hitachi TM-100, Japan) by coating with gold (two times for 10 s and 4 mA) before the imaging. The average diameter distributions of fibers were calculated using visualization software (Image J).

Laser scanning confocal microscopy

The distribution of drug in the core-shell nanofibers was studied by laser scanning confocal microscopy (LSCM). Using the mixture solution of drugs and Fluorescein isothiocyanate conjugated BSA (FITC-BSA) as inner layer, core-shell nanofibers labeled with FITC–BSA were collected on a transparent glass slide. Immediately, images of nanofibers on the glass slide were taken by Laser scanning confocal microscopy (LSCM, Carl Zeiss LSM 700, Germany) in the darkness.

Transmission electron microscopy

Transmission electron microscopy (TEM, Hitachi H-800, Japan) at 100 keV was performed to characterize the core-shell structure of co-axial electrospun nanofibers and TEM samples were prepared by collecting several bunches of fibers onto a carbon-coated Cu grid. Subsequently, TEM pictures were taken via a beam of electrons passing through the Cu grid loading the nanofibers.

Fourier transform infrared spectra

Fourier transform infrared (FTIR) spectrum of nanofibers was measured with the KBr disk method on an Avatar 380 FTIR instrument (Nicolet 6700, Thermo Fisher, USA) in order to examine the ingredient of drug-loaded nanofiber. Before the measurement, all samples were rinsed three times with pure water and treated by vacuum freeze-drying for 24 h in order to eliminate the water in nanofibers. Nanofiber sample was ground into powder with KBr for preparing a disk and subsequently spectra in transmission mode (32 scans) were recorded in the wavelength range of 4000 to 500 cm^{-1} for each sample.

Thermogravimetric analysis

The thermogravimetric analysis (TGA) was used to distinguish nanofibers composition through evaluating the decomposition temperature of nanofibers at different temperature. Specimens (5 mg in mass) were heated

from 50°C to 600°C in nitrogen atmosphere at a heating rate of 10°C min^{-1} using a thermal analyzer (TG 209 F1, Germany) and naturally cooled down to the 50°C.

Mechanical testing

Mechanical properties of drug-loaded nanofiber films were measured by a universal materials tester (H5K-S, Hounsfield, UK) as previously conducted (Jinglei Wu et al., 2014). Briefly, rectangular specimens of both ends (10 mm × 50 mm) were fixed using two grips which had a 30 mm gap between them with a load cell of 50 N and stretched with a speed of 10 mm/min at room temperature (RT) with 65% of humidity. The engineering stress was defined as the force recorded by the load cell divided by the total area of the scaffold cross section, and the strain was obtained by the ratio of scaffold elongation to the initial distance between two grips.

Drug release, degradation of nanofibers, and dissolution of gallstone in vitro

Drug release

Metal stents' coating with drug-loaded electrospun nanofiber prepared as above-mentioned parameter in Table 1 was immersed into 5 mL phosphate-buffered saline (PBS, pH 7.0) in 15 mL centrifuge tubes. Tubes with stent were immediately placed in an incubator with a shaking rate of 120 r/min at 37°C. About 1 mL releasing solution was acquired from tubes at specific time (3 h, 6 h, 9 h, 12 h, 24 h, 48 h, 72 h, 120 h, 168 h, 216 h) and an equal volume of fresh PBS was supplemented in each tube for incubation. Drugs releasing into PBS were measured by high-performance liquid chromatography (HPLC).

Degradation of nanofibers

Nanofiber film squares (20 mg in mass and 20 μm in thickness) were immersed into 20 mL PBS (pH 7.0) in 50 mL centrifuge tubes, which were placed in an undifferentiated environment as release test. Mass loss of nanofiber films after soaking for one day, two days, three days, four days, five days, one week, two weeks, one month, and two months were characterized in mass. Prior to weighing, 24-h vacuum freeze-drying procedure was utilized for eliminating water in nanofibers. The results of mass loss was expressed as the following formula: $MS(\%) = (M_0 - M_t)/M_0 \times 100$, where MS is mass loss, M_0 is the total mass of nanofiber films, and M_t is the mass of nanofiber films after soaking time t. Besides, nanofiber morphology and mechanical properties after two weeks, one month, and two months of degradation are characterized as the above-mentioned method.

Dissolution of gallstones

Gallstones (mass in 50 mg) and stents' coating with drug-loaded nanofiber films (mass in 200 mg) were placed into 10 mL PBS and the incubated condition was the same as above-mentioned in release test. Gallsotones dissolving effectiveness of stents was assessed by calculating mass loss. While stone collapsed slags or mass of gallstone unchanged over three days, test terminated.

Cytotoxicity test in vitro

Cell culture and seeding

The PIECs were incubated in high glucose Dulbecco's Modified Eagle's Medium (DMEM) containing 10% fetal bovine serum (FBS), 100 U/mL penicillin, and 100 g/mL streptomycin for cell culturing on each nanofiber samples. Core-shell drug-loaded nanofiber films (300 μm in thickness) were punched into discs (15 mm in diameter) and all disc specimens were placed at the bottom of wells in 24-well tissue culture plates (TCPs). All nanofiber samples were sterilized before cell seeding by immersing in ethanol vapor for 24 h and subsequently exposed to UV for 24 h. To remove the residual ethanol, all specimens were washed thoroughly with PBS three times. Thereafter, disc specimens were soaked into culture medium for 4 h prior to cell seeding. 1×10^4 numbers of cells were seeded in each well and incubated, and the culture plates with standard culture conditions (37°C, 5% CO_2 and 95% humidity) and growth medium were refreshed after every two days.

Cell cytotoxicity of drug-loaded nanofiber film

Cell cytotoxicity was examined by using the 3-(4,5-dimethylthiazol-2-yl)-2,5-diphenyltetrazolium bromide (MTT) to assay the cell proliferation at one, three, and five days of post seeding. After a defined time period, 40 μL of MTT solution with 360 μl of Fresh medium (without FBS) was added to the wells and incubated for 4 h at 37°C. And then culture medium with MTT solution was replaced with 400 μL of dimethyl sulfoxide (DMSO, Sinopharm, China) to dissolve the formazan crystals and incubated for 30 min at shaking incubator under the dark conditions. Finally, absorbance of the mixing solution was tested by the enzyme-labeled instrument (MK3, Thermo) at 492 nm.

Cell morphology

To observe the cell morphology, after four days of culture, mats with PIEC were rinsed with PBS to clear residual medium and fixed in 4% paraformaldehyde (Thermo Scientific) at 4°C for 30 min. After fixing, the samples were washed with PBS for three times to remove residual paraformaldehyde. Hereafter, the samples were dehydrated by using gradient ethanol from 30% to 100% concentration followed by freeze-drying overnight, and samples were observed for morphology by SEM images.

Result and discussion

Fabrication of stent coating with drug-loaded nanofiber films

Stent coating with drug-loaded nanofiber films shown in Figure 2 was produced with co-axial electrospinning process. In terms of co-axial electrospinning, the stability of Taylor's cone structured with two-layer droplets is strongly affected by the physical properties of solutions (viscosity, core/sheath interface tension).[33] Besides, when the injected rate of shell layer is a fixed value, nanofiber core-shell structure is also affected by the injected rate of core layer. Presently, by regulating different injected rate in core layer, core-shell nanofiber films loaded with different amounts of drugs were fabricated and the injected rates of two layers are summarized in Table 1. Fiber morphology characterized by SEM is shown in Figure 3. Average diameter of PLCL-D-10 and PLCL-D-30 is 1146.79 ± 433.02 nm (Figure 3(g)) and 1531.22 ± 481.46 nm (Figure 3(h)), respectively, which is close to the diameter of PLCL-W nanofibers (Figure 3(f)) (1461.54 ± 612.64 nm) but is more than diameter of pure PLCL nanofibers produced by uniaxial electrospinning because of existence of core-shell structure. When the injected rate of core layer increases to over 0.4 mL/h, the microstructure of nanofibers changes significantly. It is observed from SEM images (Figure 3(i) and (j)) that single fibers aggregate and bond together as fiber bundles with large diameter with tens of micrometer. Nanofibers with core-shell structure possess larger diameter than nanofibers fabricated by uniaxial electrospinning is also reported by He et al.[34] in previous research. As a consequence of PLCL, nanofiber films shrink after HPIF volatilizing, and lumen diameter of coated stent given in Table 2 slightly decrease.

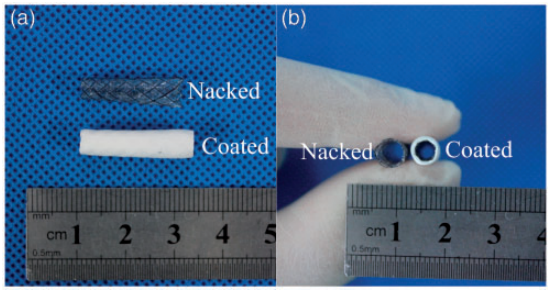

Figure 2. Digital picture of naked stent and coated stent. (a) Front view and (b) lateral view.

The core-shell structure of fibers observed by LSCM and TEM images proves to contain ECTA&SC in fibers. In Figure 4(a), the mixture of drug and FITC–BSA-loaded nanofibers emits green fluorescent light in interior part of fibers, indicating that the core-shell structure existed in nanofibers. Furthermore, core-shell structures of fibers are clearly and directly demonstrated by TEM micrograph in Figure 4(b).

ATR-FTIR and TGA are more intuitive evidences for ECTA&SC being loaded into nanofibers. As shown in ATR-FTIR spectra (Figure 5(a)), O = S = O peaks at 1180 cm^{-1} (blue arrow) and –OH peaks at 3200 cm^{-1} to 3500 cm^{-1} (red arrow) merely exhibit in pure SC while they are not shown in pure PLCL polymer and EDTA. O = S = O and –OH characteristic peaks observed in Drug-10 and Drug-60 give an evidence of ECTA&SC successfully loaded into fibers. Peaks of methyl at 2800 cm^{-1} to 3200 cm^{-1} (dash oval) increasing also demonstrate the presence of ECTA&SC in nanofibers. There are not enough characteristic peaks to prove EDTA existence due to all functional group peaks overlapping with PLCL and SC. But conclusion of EDTA presence in fibers could be obtained from TGA curve (Figure 5(b)). The significant evidence for EDTA observed in Figure 5(b) is that decomposition temperature of pure EDTA, PLCL-D-10, and PLCL-D-60 starts at 242°C but pure PLCL and pure SC separately occur at 300°C and 370°C. Another proof for SC is that curves of pure PLCL and pure EDTA display a plain trend at 428°C, while PLCL-D-10, PLCL-D-60, and pure SC still present decreasing trend.

The mechanical behavior of nanofiber is an essential factor for its effective application as a coating film in the field of biomedical engineering. Stress–strain curve (Figure 6(a)) presents that all specimens exhibited linear elastic performance. In Figure 6(b), it showed that there are unobovious changes in tensile strength, while elongation at break (Figure 6(c)) of PLCL-D-10, PLCL-D-30 and PLCL-D-50 was lower than PLCL-W. It is shown in Figure 6(d) that the value of Young's modulus of drug-loaded nanofibers enlarged in varying degrees. The result of mechanical behavior indicates that ECTA&SC enhance the stiffness but reduce elasticity of PLCL nanofibers. Overall, mechanical changes have no effect on its application as a coated film.

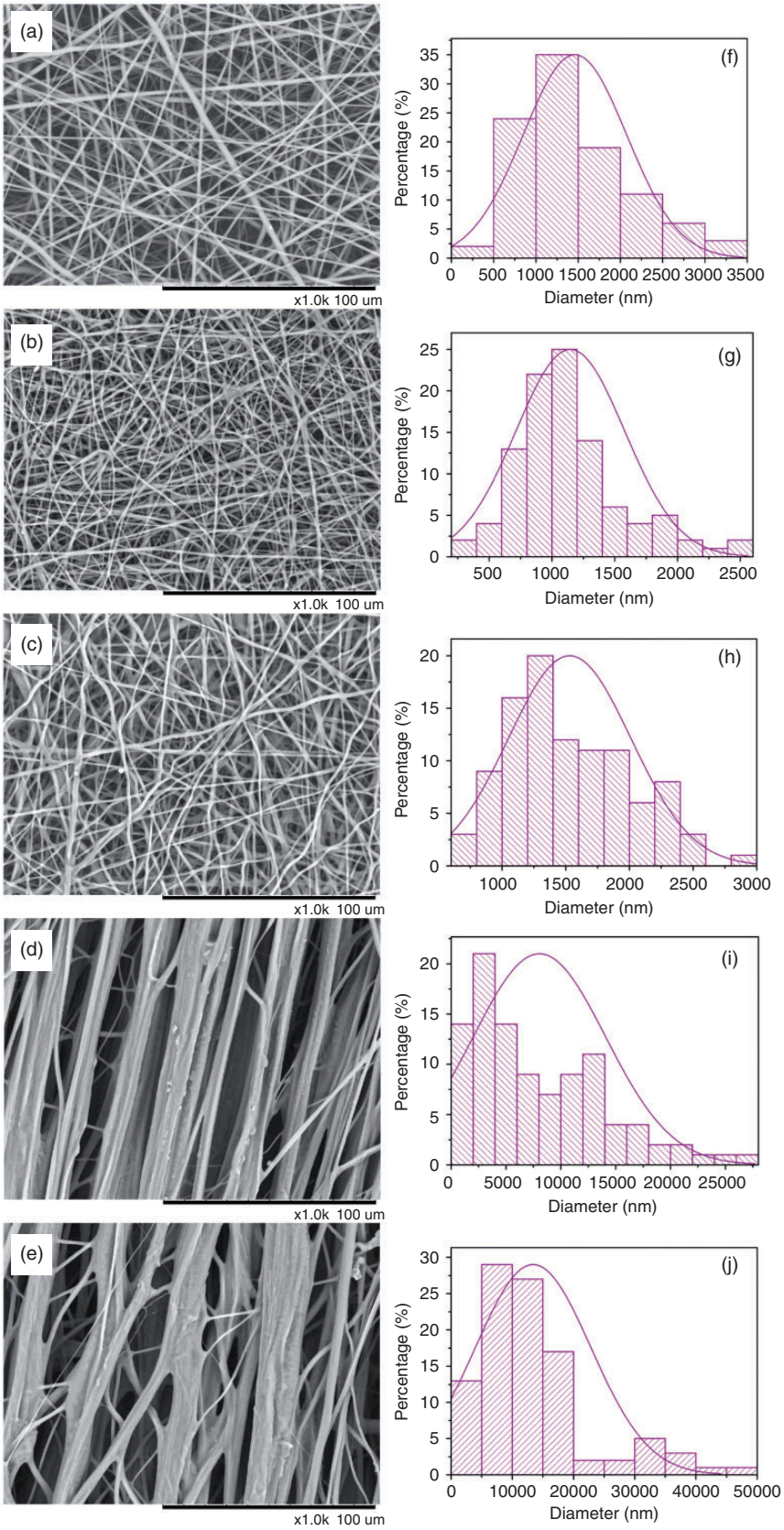

Figure 3. SEM images of PLCL-W (a), PLCL-D-10 (b), PLCL-D-30 (c), PLCL-D-50 (d) and PLCL-D-60 (e) and their distribution diameter diagrams of nanofibers (f to j).

Drug release and degradation of nanofibers in vitro

Drug release behaviors of stents coating with PLCL-D-10, PLCL-D-30, PLCL-D-50, and PLCL-W specimens are characterized by using HPLC to measure the content of EDTA&SC in PBS after fixed time. The drug release curve of stents shown in Figure 7 is acquired at fixed points of time (3 h, 6 h, 9 h, 12 h, 24 h, 48 h, 72 h, 120 h, 168 h, and 216 h). As seen in Figure 7, significant burst release phenomenon exists in all drug-loaded nanofiber samples after soaking for 12 h initially, and cumulative release amount of EDTA&SC is nearly 50–80% of total amount loaded in nanofibers. The following three reasons can explain the serious burst release: (1) EDTA&SC with negative charges easily transfer to the surface of nanofibers during electrospinning process, staying on the surface of shell rather than in the inner layer; (2) core layer with high injected rate cannot be enwrapped by shell PLCL layer, forming opening slit connected core with external environment; (3) PLCL nanofiber absorb water and then swell to form wet channels[35] in shell layer, distributing water-soluble EDTA&SC molecular into surroundings easily. At the end of the initial 12-h burst release, EDTA&SC release rate decreases and achieves a stable of zero-release phase. It can be seen in Figure 7 that drug releasing time decreases with the increasing amount of EDTA&SC in nanofibers and, respectively, are 168 h (PLCL-D-10), 120 h (PLCL-D-30), and 72 h (PLCL-D-50). In contrast, no trace is signed in the sample of PLCL-W.

Table 2. Lumen diameter of stent.

Stent type	Great end (mm)	Small end (mm)
Naked stent	5.62 ± 0.06	4.24 ± 0.52
Coated stent	4.71 ± 0.04	3.35 ± 0.34

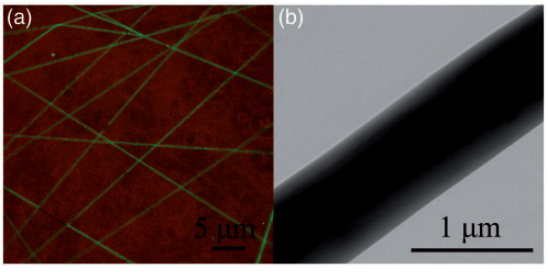

Figure 4. (a) LSCM image of electrospun nanofibers loaded with the mixture of ECTA&SC and FITC-BSA, (b) TEM photograph of nanofibers loaded with ECTA&SC.

The degradation of drug-loaded nanofiber, when samples are incubated into PBS at 37°C, is evaluated by film mass loss and nanofiber morphology using SEM images. As can be seen in Figure 8, rapid mass loss of all drug-loaded nanofiber films occurs within the initial period of seven days apart from PLCL-W sample due to drugs release from nanofibers instead of PLCL degradation because mass loss percent of PLCL-W without drugs is merely $0.56\% \pm 1.14\%$. In the latter period of 7 days to 60 days, extremely slow ascension of all nanofibers is exhibited in mass loss curve due to PLCL material degradation. Compared to PLDL-W, the same degraded trend of all drugs-loaded nanofibers reveals that EDTA&SC loaded in nanofiber have no effect on PLCL degradation.

Biomaterial degradation test in vitro is essential for clinical application and morphology change of fiber is a common method for evaluating the degree of degradation. SEM image displayed in Figure 9 shows the morphology of nanofibers after degradation in PBS at 37°C for a period of 2 weeks, 4 weeks and 8 weeks separately. Good fiber morphology and slight swelling effects are displayed in all nanofibers shown in Figure 9

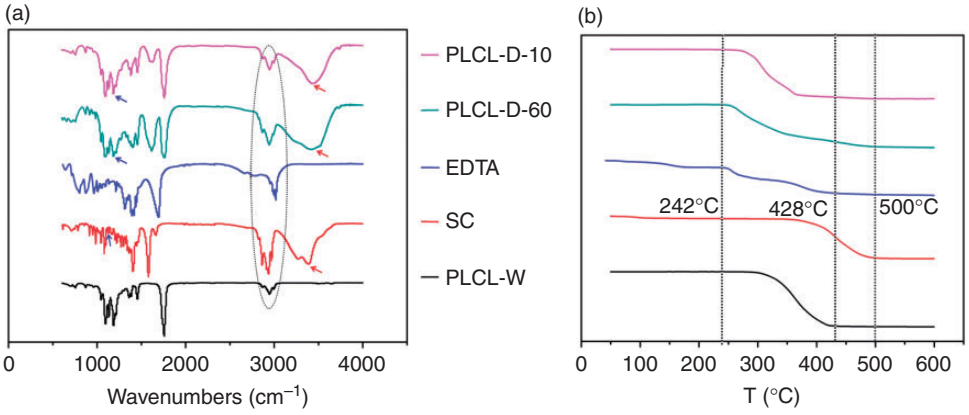

Figure 5. ATR-FTIR spectra (a) and TGA curve (b) of electrospun nanofiber loaded with different amount of ECTA&SC.

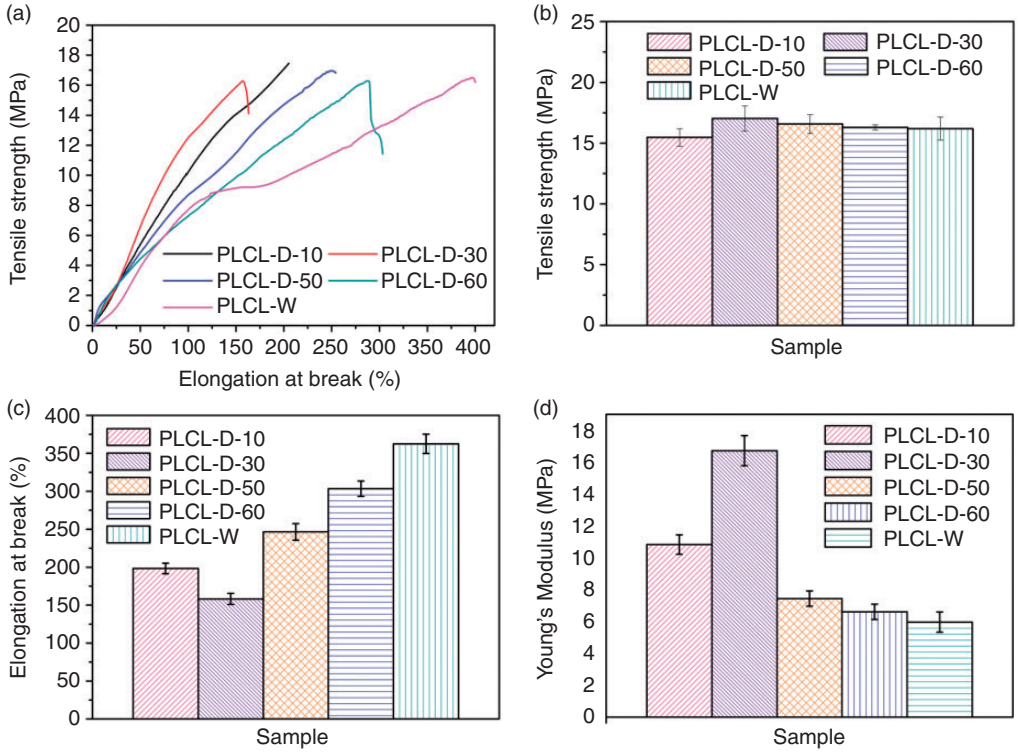

Figure 6. Mechanical properties of nanofibers loaded with different amount of drugs. (a) Stress–strain curves, (b) tensile strength, (c) elongation at break, and (d) Young's modulus.

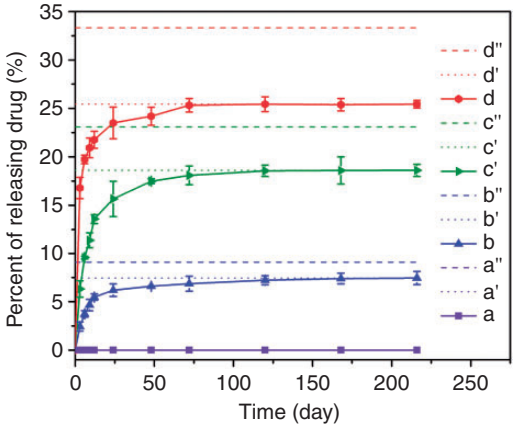

Figure 7. Drug release curve of stent coating with drug-loaded nanofibers. Actual releasing amount of stent coating with PLCL-W (a), stent coating with PLCL-D-10 (b), stent coating with PLCL-D-30 (c), stent coating with PLCL-D-50 (d) and total drug releasing amount after two months of incubation of stent coating with PLCL-W (a′), stent coating with PLCL-D-10 (b′), stent coating with PLCL-D-30 (c′), stent coating with PLCL-D-50 (d′) and theoretical value of drug in stent coating with PLCL-W (a″), stent coating with PLCL-D-10 (b‴), stent coating with PLCL-D-30 (c″), stent coating with PLCL-D-50 (d″).

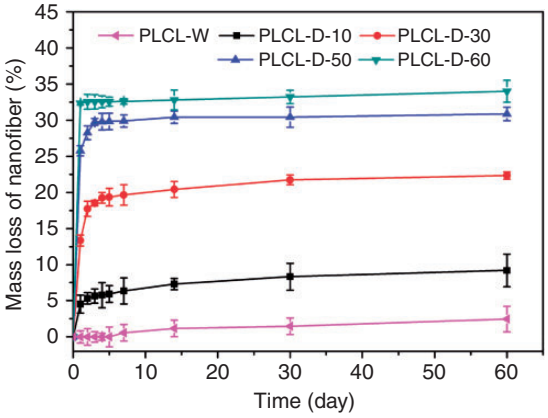

Figure 8. Mass loss curve of nanofiber films loaded with different amount of drug.

after two months of degradation. As shown in Figure 10, mechanical property of all samples, including Young's modulus, tensile strength and elongation at break, significantly change over the time passing by. Degraded effect of nanofibers result in decreasing of tensile strength, given in Figure 10(a). Interestingly, after two months of immersing in PBS, 10%, 32%,

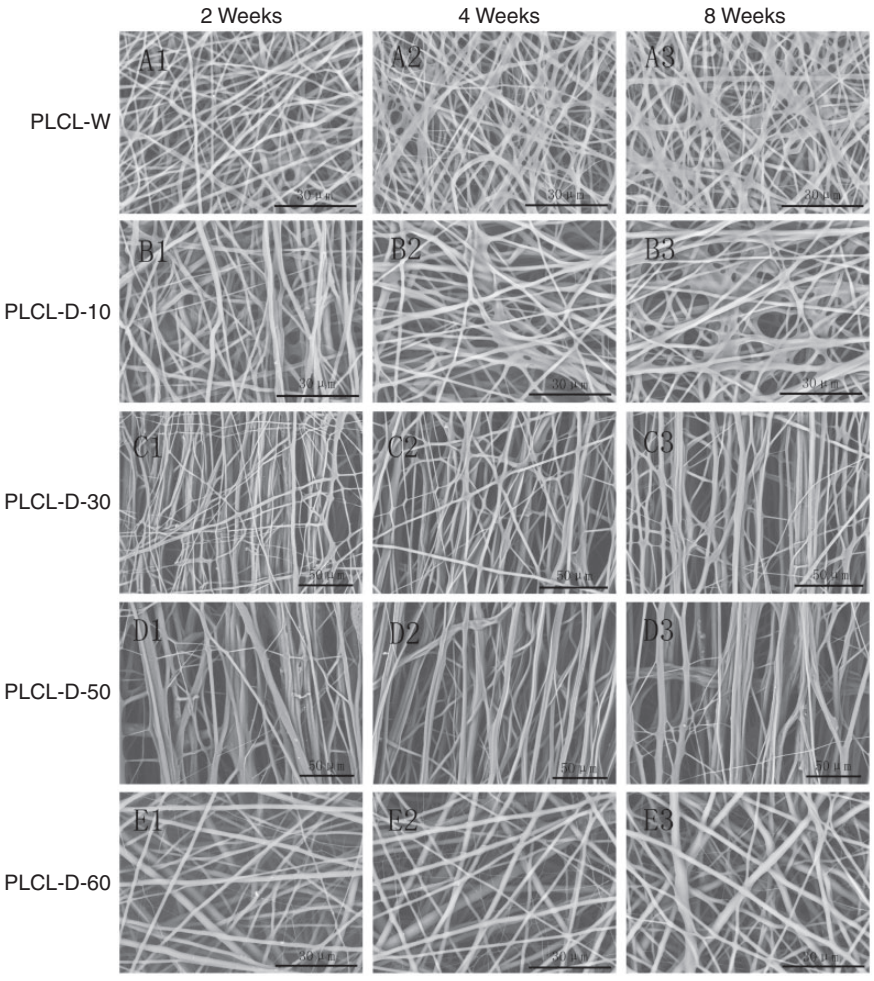

Figure 9. Morphology of nanofiber loaded different amount of drugs at different degraded time.

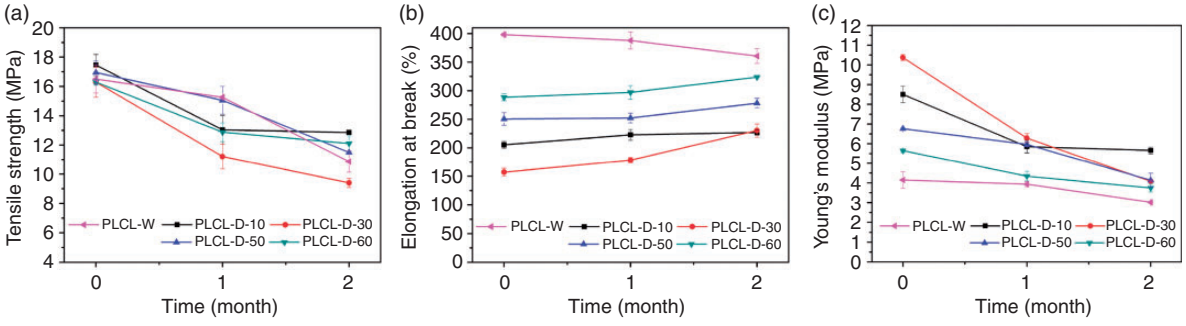

Figure 10. Mechanical properties during the period of degradation of nanofibers. (a) Young's modulus, (b) tensile strength, and (c) elongation at break.

10%, and 11% increment was exhibited as shown in Figure 10(c) in Drug-10, Drug-30, Drug-50, and Drug-60, correspondingly. Whereas, Young's modulus (Figure 10(a)), respectively, decreases in the first incubated month from 8.50 ± 0.41 MPa to 5.85 ± 0.31 MPa (Drug-10), 10.37 ± 0.15 MPa to 6.29 ± 0.22 MPa (Drug-30), 6.76 ± 0.05 MPa to 5.96 ± 0.12 MPa (Drug-50) and 5.65 ± 0.10 MPa to 4.34 ± 0.25 MPa (Drug-60) due to drug molecule dissolved out from core-shell nanofibers to surroundings. PLCL nanofibers releasing drugs out became soft and elastic. After another one month, there was continuous reduction in Young's modulus to 5.66 ± 0.17 MPa (Drug-10), 4.08 ± 0.02 MPa (Drug-30), 4.13 ± 0.35 MPa (Drug-50), and 3.74 ± 0.20 MPa

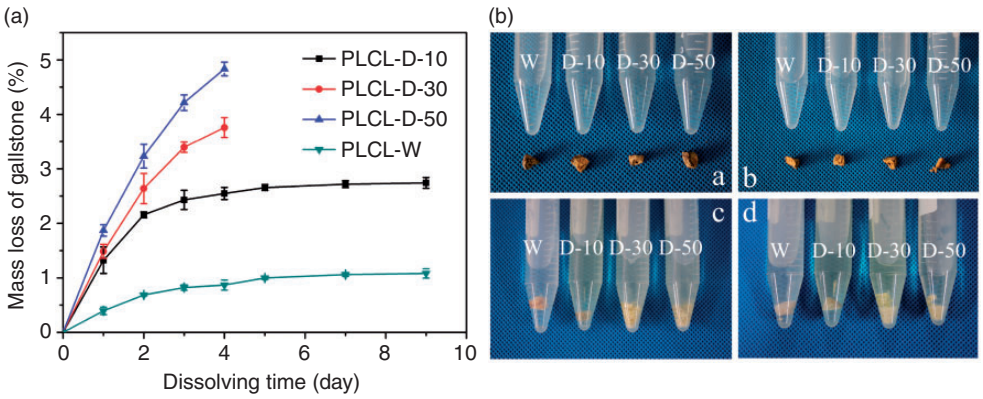

Figure 11. (a) Mass loss curve of gallstones immersing in PBS with stents loaded different amount of drugs, (b) digital photographs of gallstone dissolving effectiveness after 0 day (a), 2 days (b), 5 days (c) and 7 days (d). (D-N, D-10, D-30, and D-50 correspondingly represented gallstone soaking with stent coated film of PLCL-W, PLCL-D-10, PLCL-D-30, and PLCL-D-50.)

(Drug-60) caused by PLCL polymer degradation. In summary, drug molecule loaded in nanofiber will affect PLCL polymer mechanical behavior but does not change the degrading process of PLCL nanofibers. Importantly, all nanofiber films after two months of degradation still firmly wrapped on the stent and no shedding results occurred.

The gallstone mass loss curve reveals that four kinds of stents coated with nanofiber films loaded with different amount of drugs have different dissolution effects. As shown in Figure 11(a), mass loss percentage of gallstone in stent coating with PLCL-W sample is merely $1.08\% \pm 0.08\%$ after nine days of incubation, which can be attributed to gallstone swelling in PBS and some water-soluble substance dissolving out. In stent coating with PLCL-D-10, the mass of stone stopped decreasing after five days of soaking with stent coating with PLCL-D-10 nanofibers in PBS and gallstone is dissolved by $2.74 \pm 0.10\%$ due to drugs released out from nanofibers as shown in releasing result. Perfect results of gallstone dissolution are obtained from stent coating with PLCL-D-30 and stent coating with PLCL-D-50 in the media of PBS with gallstone that total mass loss is $3.76 \pm 0.18\%$ and $4.83 \pm 0.12\%$, separately. More importantly, gallstones soaking with stent coating with PLCL-D-30 and stent coating with PLCL-D-50 break into small pieces and the initial integrated morphology disappears totally. In Figure 11(Bb), it can be observed that small fragments detach from gallstone after two days soaking with stent coating with PLCL-D-50. Moreover, after immersing for five days in PBS, gallstone soaking with stent coating with PLCL-D-30 and stent coating with PLCL-D-50 completely broke down into small pieces, but debris of gallstone are much tinner in D-50 than that in D-30 (Figure 11 (Bc)). Finer debris is obtained after seven days of soaking with stent coating with PLCL-D-30 and stent coating with PLCL-D-50.

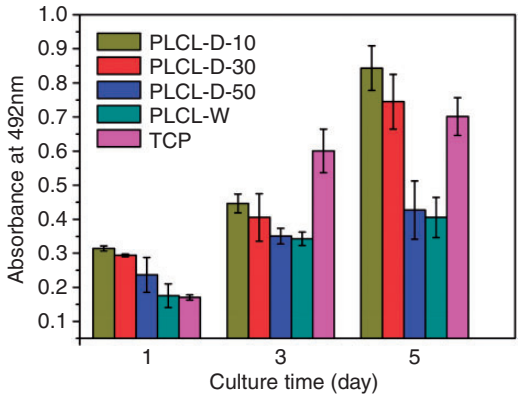

Figure 12. MTT essay of PIECs, respectively, cultured for one, three, and five days on nanofiber films loaded with different amount of drug.

Cytotoxicity test in vitro

The PIECs were seeded onto core-shell nanofiber membranes at a density of 5×10^3 cells/well in 24-well TCP to assess the cytotoxicity by MTT. Proliferation of PIECs was studied up to five days and viability of cells after seeding was investigated at one, three, and five days by detecting absorbance of each well at 492 nm. The result shown in Figure 12 demonstrates that PIECs can regularly be proliferated on all nanofiber samples by culturing for five days and further indicated that EDTA&SC are non-toxic and supported to PIECs as compared to PLCL-W. An interesting phenomenon can be observed that PIECs had a higher growth rate on PLCL-D-10 and PLCL-D-30 nanofiber

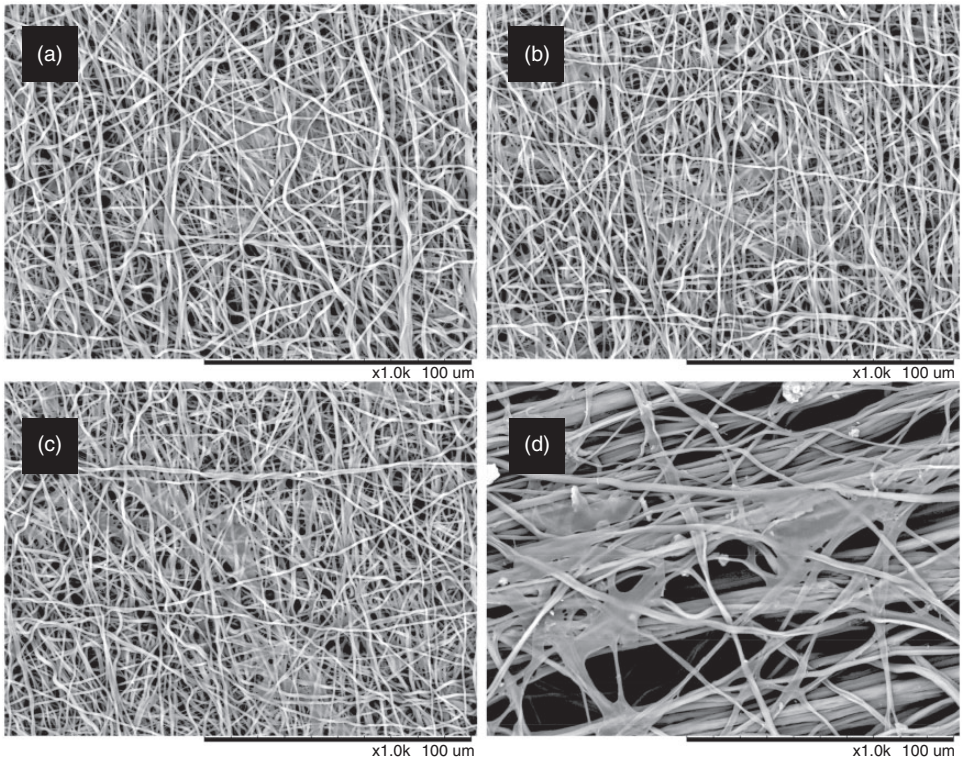

Figure 13. Morphology of PIECs cultured for three days on nanofiber films of PLCL-W (a), PLCL-W-10 (b), PLCL-D-30 (c), and PLCL-D-50 (d).

films. Absorbance at 492 nm of PLCL-D-10 on the fifth day is almost as double as PLCL-W, which indicates that minute quantity of EDTA&SC can accelerate PIECs proliferation due to the inhibited effect eliminated among cells because EDTA can chelate Ca^{2+} to deactivate protein. SEM images shown in Figure13 indicate that PIECs can spread, attach, and reproduce on all nanofiber mats.

Conclusions

Stent insertation technology has become a common means of treating CBD disease. Here metal stent coating with core-shell nanofiber films loaded with EDTA&SC was fabricated by co-axil electrospinning for dissolving gallstone and dredging biliary. LSCM and TEM images prove that core-shell structure existence in fibers produced by co-axial electrospinning. ATR-FTIR spectrum and TGA curve confirm the truth of loaded EDTA&SC in fiber. In vitro release test, EDTA&SC are continuously released from stents coating with drug-loaded nanofiber film for around 5 days and burst release exists in all specimens at initial period attributed to EDTA&SC being easily water-soluble. The breaking of gallstones demonstrates that this stent has a dissolving effect on gallstone. Moreover, non-cytotoxicity is concluded from MTT result. Although perfect effect has been proved in vitro, it is still unclear for its dissolving effect in complex vivo environment. We convince that this stent coating with nanofiber film loaded with EDTA&SC is a potentially novel method for curing gallstone disease, but further study on clinical research is imperative in future.

Authors' contribution

QG and CH contributed equally to this work.

Declaration of Conflicting Interests

The author(s) declared no potential conflicts of interest with respect to the research, authorship, and/or publication of this article.

Funding

The author(s) disclosed receipt of the following financial support for the research, authorship, and/or publication of this article: This work was supported by the National Natural Science Foundation of China (grant no. 81470904). The authors would like to extend their sincere appreciation for the guidance of supervisor Prof. Mo and assistance from all members of biomaterial and tissue engineering group in DongHua University.

References

1. Hochberger J, Tex S, Maiss J, et al. Management of difficult common bile duct stones. *Gastrointest Endosc Clin N Am* 2003; 13: 623–634.
2. Kim HJ, Choi HS, Park JH, et al. Factors influencing the technical difficulty of endoscopic clearance of bile duct stones. *Gastrointest Endosc* 2007; 66: 1154–1160.
3. Tint GS, Salen G, Colalillo A, et al. Ursodeoxycholic acid: a safe and effective agent for dissolving cholesterol gallstones. *Ann Intern Med* 1982; 97: 351–356.
4. Katsinelos P, Kountouras J, Paroutoglou G, et al. Combination of endoprostheses and oral ursodeoxycholic acid or placebo in the treatment of difficult to extract common bile duct stones. *Digest Liver Dis* 2008; 40: 453–459.
5. Leuschner U, Sieratzki J, Klempa I, et al. Investigations on the toxicity of bile salt solutions, Capmul 8210 and a bile salt-EDTA solution for common bile duct perfusion in dogs. *Digestion* 1984; 30: 23–32.
6. Hong WD, Zhu QH and Huang QK. Endoscopic sphincterotomy plus endoprostheses in the treatment of large or multiple common bile duct stones. *Digest Endosc: official journal of the Japan Gastroenterological Endoscopy Society* 2011; 23: 240–243.
7. Cai XB, Zhang WX, Wan XJ, et al. The effect of a novel drug-eluting plastic stent on biliary stone dissolution in an ex vivo bile perfusion model. *Gastrointest Endosc* 2014; 79: 156–162.
8. Cai XB, Zhang WX, Zhang RL, et al. Safety and efficacy of a novel plastic stent coated with stone-dissolving agents for the treatment of biliary stones in a porcine model. *Endoscopy* 2015; 47: 457–461.
9. Bhardwaj N and Kundu SC. Electrospinning: a fascinating fiber fabrication technique. *Biotechnol Adv* 2010; 28: 325–347.
10. Luo CJ and Edirisinghe M. Core-liquid-induced transition from coaxial electrospray to electrospinning of low-viscosity poly(lactide-co-glycolide) sheath solution. *Macromolecules* 2014; 47: 7930–7938.
11. Chen M, Wang CJ, Fang W, et al. Electrospinning of calixarene-functionalized polyacrylonitrile nanofiber membranes and application as an adsorbent and catalyst support. *Langmuir* 2013; 29: 11858–11867.
12. Carson D, Jiang Y and Woodrow KA. Tunable release of multiclass anti-HIV drugs that are water-soluble and loaded at high drug content in polyester blended electrospun fibers. *Pharmaceut Res* 2016; 33: 125–136.
13. Lomov SV and Molnar K. Compressibility of carbon fabrics with needleless electrospun PAN nanofibrous interleaves. *Express Polym Lett* 2016; 10: 25–35.
14. Hu J, Prabhakaran MP, Tian LL, et al. Drug-loaded emulsion electrospun nanofibers: characterization, drug release and in vitro biocompatibility. *Rsc Adv* 2015; 5: 100256–100267.
15. Chen GY, Xu Y, Yu DG, et al. Structure-tunable Janus fibers fabricated using spinnerets with varying port angles. *Chem Commun* 2015; 51: 4623–4626.
16. Ryu J, Choi S, Bok T, et al. Nanotubular structured Si-based multicomponent anodes for high-performance lithium-ion batteries with controllable pore size via coaxial electro-spinning. *Nanoscale* 2015; 7: 6126–6135.
17. Wu J, Huang C, Liu W, et al. Cell infiltration and vascularization in porous nanoyarn scaffolds prepared by dynamic liquid electrospinning. *J Biomed Nanotechnol* 2014; 10: 603–614.
18. An S, Jo HS, Song KY, et al. Electrically-charged recyclable graphene flakes entangled with electrospun nanofibers for the adsorption of organics for water purification. *Nanoscale* 2015; 7: 19170–19177.
19. Chen JY, Wu HC, Chiu YC, et al. Plasmon-enhanced polymer photovoltaic device performance using different patterned Ag/PVP electrospun nanofibers. *Adv Energy Mater* 1996; 4(8): 6510–6510.
20. Li XD, Gao CT, Duan HG, et al. High-performance photoelectrochemical-type self-powered UV photodetector using epitaxial TiO_2/SnO_2 branched heterojunction nanostructure. *Small* 2013; 9: 2005–2011.
21. Cestari M, Muller V, Rodrigues JHD, et al. Preparing silk fibroin nanofibers through electrospinning: further heparin immobilization toward hemocompatibility improvement. *Biomacromolecules* 2014; 15: 1762–1767.
22. Xue R, Nelson MT, Teixeira SA, et al. Cancer cell aggregate hypoxia visualized in vitro via biocompatible fiber sensors. *Biomaterials* 2016; 76: 208–217.
23. Zhu X, Ni S, Xia T, et al. Anti-neoplastic cytotoxicity of SN-38-loaded PCL/Gelatin electrospun composite nanofiber scaffolds against human glioblastoma cells in vitro. *J Pharmaceut Sci* 2015; 104: 4345–4354.
24. Merkle VM, Tran PL, Hutchinson M, et al. Core-shell PVA/gelatin electrospun nanofibers promote human umbilical vein endothelial cell and smooth muscle cell proliferation and migration. *Acta Biomater* 2015; 27: 77–87.
25. Kijenska E, Prabhakaran MP, Swieszkowski W, et al. Interaction of Schwann cells with laminin encapsulated PLCL core-shell nanofibers for nerve tissue engineering. *Eur Polym J* 2014; 50: 30–38.
26. Liu GY, Tang Q, Yu YN, et al. Electrospun core-sheath fibers for integrating the biocompatibility of silk fibroin and the mechanical properties of PLCL. *Polym Adv Technol* 2014; 25: 1596–1603.
27. Kim EJ, Jeon EK and Baek K. Role of reducing agent in extraction of arsenic and heavy metals from soils by use of EDTA. *Chemosphere* 2016; 152: 274–283.
28. Chauque EFC, Dlamini LN, Adelodun AA, et al. Modification of electrospun polyacrylonitrile nanofibers with EDTA for the removal of Cd and Cr ions from water effluents. *Appl Surf Sci* 2016; 369: 19–28.
29. Lima-Oliveira G, Salvagno GL, Danese E, et al. Sodium citrate blood contamination by K2 -ethylenediaminetetraacetic acid (EDTA): impact on routine coagulation testing. *Int J Lab Hematol* 2015; 37: 403–409.
30. Dai KY, Montet JC, Zhao XM, et al. Dissolution of human brown pigment biliary stones. *J Hepatol* 1989; 9: 301–311.
31. Lin XZ, Lin CY, Chang TT, et al. Choledocholithiasis treated by ethylenediaminetetraacetic acid infusion through an endoscopic nasobiliary catheter. *J Gastroen Hepatol* 1992; 7: 335–338.

32. Sohrabi A, Max MH and Hershey CD. Cholate sodium infusion for retained common bile duct stones. *Archive Surg* 1979; 114: 1169–1172.
33. Ramakrishna S. *An introduction to electrospinning and nanofibers*. Hackensack, NJ: World Scientific, 2005.
34. He M, Xue JJ, Geng H, et al. Fibrous guided tissue regeneration membrane loaded with anti-inflammatory agent prepared by coaxial electrospinning for the purpose of controlled release. *Appl Surf Sci* 2015; 335: 121–129.
35. Han D and Steckl AJ. Triaxial electrospun nanofiber membranes for controlled dual release of functional molecules. *Acs Appl Mater Int* 2013; 5: 8241–8245.